Published in: Chemical Physics (2000), vol. 260, pp. 237-243.
Status: Postprint (Author's version)

The photoabsorption and constant ionic state spectroscopy of vinylbromide

A. Hoxha [a], R. Locht [a], B. Leyh [a, 1], D. Dehareng [b], K. Hottmann [c], H. W. Jochims [c], H. Baumgärtel [c]

[a] *Département de Chimie Générale et de Chimie Physique, Institut de Chimie Bât. B6c, Université de Liège, par B-4000 Sart-Tilman, Liège 1, Belgium*
[b] *Centre d'Ingéniérie des Protéines, Bât. B6a, Université de Liège B-4000 Sart-Tilman, Liège 1, Belgium*
[c] *Institut für Physikalische und Theoretische Chemie, Freie Universität Berlin, Takustraße 3, D-14195 Berlin, Germany*

Abstract

In this paper, we report the photoabsorption and the constant ionic state spectroscopy of vinyl bromide (C_2H_3Br). The photoabsorption spectrum was measured using synchrotron radiation and was investigated in detail between 5.0 and 12.0 eV photon energy revealing many previously unobserved structures. These features were analyzed in terms of valence to virtual valence transitions and Rydberg series. The examination of the three Rydberg series converging towards the first ionization threshold (2a" → *n*s, 2a" → *n*p and 2a" → *n*d) leads to wave numbers of 335 ± 30, 690 ± 30 and 1305 ± 30 cm^{-1}. The vibrational wave numbers of the progressions belonging to Rydberg series converging towards the second ionization threshold are 485 ± 30 and 1145 ± 50 cm^{-1}. Ab initio calculations helped the assignment of the valence transitions and of the observed vibrational wave numbers in the Rydberg series.

Constant ionic state spectra were recorded for vibronic states corresponding to the first and the second electronic states of the ion. Their fine structures are assigned to the autoionization of Rydberg states. The autoionization decay of these Rydberg states is analyzed qualitatively in terms of the vibrational nature of the final ionic state.

1. Introduction

In a previous paper on the spectroscopy of vinyl bromide [1] we analyzed the He(I) photoelectron and threshold photoelectron spectra. In this second contribution, we are mainly concerned with the photoabsorption and constant ionic state (CIS) spectroscopy of this molecular species. We will report here on the photoabsorption spectrum between 5 and 20 eV photon energy, focusing on the 5-12 eV region. The CIS spectra will also be analyzed, focusing on the autoionization decay channels of the Rydberg states involved. The closely related photoion spectroscopy has been measured in the same region of interest and will be reported later. On the other hand, the dynamics of the bromine loss from the $C_2H_3Br^+$ ion has been analyzed in detail in a recent publication [2].

The vacuum UV photoabsorption spectrum of C_2H_3Br in the 6-11 eV range has first been studied by Schander and Russel in 1975 [3]. Nearly at the same time Lohr et al. [4] reported the UV spectrum in the 8.5-11 eV region and the low resolution photoionization efficiency curves of $C_2H_3Br^+$, $C_2H_3^+$, $C_2H_3^+$, HBr^+ and Br^+. Sze et al. [5] have also investigated this molecule by electron energy loss spectroscopy both in the inner shell and valence shell energy region. However, due to the limited resolution of these works, the observed fine structures could not be properly analyzed. On the other hand, the only theoretical work on the excited states of the neutral molecule has been performed by Michl [6]. To the best of our knowledge, the CIS spectra of the $C_2H_3Br^+$ vibronic states have never been reported earlier.

2. Experimental

In the experiments reported here, we used the vacuum UV light from the synchrotron radiation provided by the electron storage ring BESSY (Berlin). The photoabsorption experimental setup, presented in Fig. 1, will be described in detail in a further publication. We will only give here the most salient features. The VUV monochromator (1 m-NIM-2 beamline) is a modified M-225 McPherson with 1.5 m focal length (instead of 1 m for the original version). A laminar Zeiss grating is used for efficient reduction of the second-spectral order (1200 lines per mm gold coated). The light passes a 1 mm thick stainless steel microchannel plate (needed for pressure reduction of 1:1000) before entering a 30 cm long stainless steel absorption cell. The vapor pressure is precisely measured by a Balzers capacitance manometer head. From Beer's law the absolute photoabsorption coefficients could be determined (after linear extrapolation to 760 Torr and 273 K). The small pressure gradient inside the absorption cell due to the gas leak through the microchannel plate has not been taken into account in the cross-section determination. One scan with gas and another empty cell run were needed for one spectrum.

[1] Chercheur qualifié du F.N.R.S. (Belgium).

The high stability of the synchrotron radiation and temperature stabilization of the sample container guarantee reliable experimental data evaluation. The two entrance and exit slits were 100 μm wide which gave about 0.1 nm wavelength resolution. Light detection was provided by a sodium salicylate sensitized photomultiplier. The photon energy scale of the monochromator is calibrated at the zero order and checked with the Ar absorption spectrum.

Fig. 1. *Schematic representation of the experimental setup used for photoabsorption.*

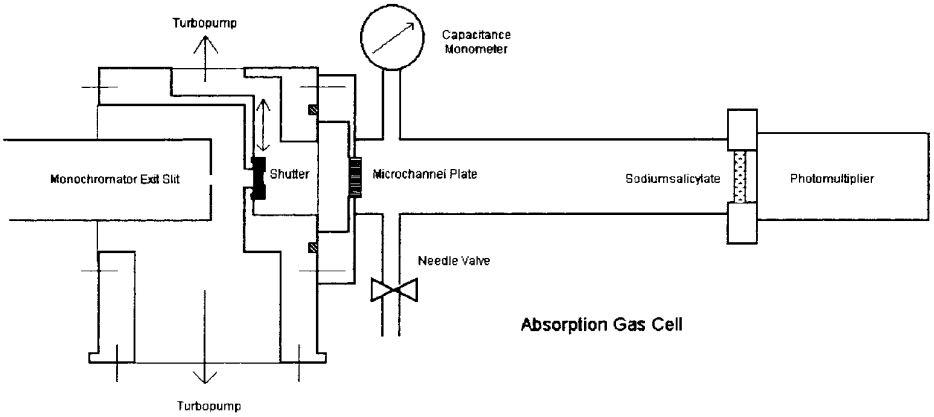

Details of the other experimental setup, used for the CIS spectroscopy, have been outlined earlier [7,8]. Briefly, the light dispersed by a 3 m normal incidence monochromator (3 m-NIM-1 beamline) is focused into an ion chamber, in the focusing plane of a tandem electron spectrometer consisting in two 180° electrostatic deflectors. The transmission function of the monochromator is measured by the photoelectron signal of a gold diode inserted in the ion chamber at the opposite of the monochromator exit slit. The constant ion state spectroscopy provides the relative partial ionization cross-sections as a function of the photon energy for well-defined electronic and/or vibrational states of the molecular ion under investigation. For recording these spectra, the photon energy $h\nu$ and the photoelectron kinetic energy E_{kin}^{e} are scanned in parallel in order to keep the energy difference $h\nu - E_{kin}^{e}$ = IE constant, i.e., the ionization energy corresponding to the selected ionic state.

The photon energy scale of the monochromator is calibrated with rare gas (Ar or Xe) threshold photoelectron spectra. In order to obtain the relative partial cross-sections, the photoelectron signals measured in the CIS spectra are normalized for the transmission functions of the monochromator and the electron energy analyzer. The former is given by the photoelectron signal of the gold diode (see above) while the latter is obtained by recording the unstructured CIS curve of Xe^{+} ($^{2}P_{1/2}$) in the region of interest. Both are previously normalized to the synchrotron beam intensity. For the present experiment, the monochromator entrance and exit slit widths are set at 200 μm.

The C_2H_3Br sample used in these experiments, purchased from Aldrich Chem. Inc. (98% purity, inhibited with 200 ppm monoethyl ether hydro-quinone), is used without further purification.

3. Computational tools

In order to help with the assignment of the first valence bands in the photoabsorption spectrum, we performed some ab initio calculations. All the calculations were performed with GAUSSIAN 94 [9], on two computers, a Dec 8400 with eight processors, and a Dec 4100 with four processors. The calculation levels used were the following: the multiconfigurational self-consistent field (SCF) level named complete active space SCF (CASSCF) [10] and the configuration interaction expansion on all the single substitutions (CIS) [11]. The basis set used was 6-311G [12] with diffuse (+) [13] and polarization (*) [14] functions on the heavy nuclei, labeled 6-311+G*. In the following, the CASSCF calculations are denoted CAS(ne, *n*MO), where ne and *n*MO are, respectively, the active electrons and active molecular orbitals (MO) numbers.

The ground electronic state geometry of the neutral molecule was optimized at the CAS-SCF(8,7) level. The excited states of the neutral were determined at the CASSCF(8,7) level, with an averaging of the molecular orbitals on all the considered states. In order to assign the observed bands to the related states, the oscillator strengths of the transitions were calculated at the CIS level. At this level, the relative position of the excited states are not necessarily reproduced but the magnitude of the calculated transition oscillator strength is very helpful.

Published in: Chemical Physics (2000), vol. 260, pp. 237-243.
Status: Postprint (Author's version)

4. Experimental results

4. 1. The absorption spectrum

The vacuum UV photoabsorption spectrum, recorded between 5.0 and 20.0 eV is shown in Fig. 2a. Fig. 2b and c display the 5-12 eV region in an expanded photon energy scale. In comparison with the spectra described in the literature [3-5] many additional previously unresolved structures are observed, e.g. in the energy region around 8.5 eV or in the 10-11 eV photon energy range. In addition, some other features can be seen in the less structured higher energy region. The relatively broad band located at about 16.8 eV corresponds to an autoionizing state that might be involved in the dissociation mechanism of $C_2H_3Br^+$ ions produced by the Ne(I) resonance line [2]. In order to better visualize it, Fig. 2a also displays the 13-18 eV region in an extended scale.

Fig. 2. *(a) The overall photoabsorption spectrum of C_2H_3Br recorded between 5.0 and 20.0 eV. The position of the main broad bands assigned as valence to virtual valence transitions are indicated by letters A to E. (b and c) The photoabsorption spectrum of C_2H_3Br recorded between 5.0 and 11.0 eV. Interpretation and assignments in terms of Rydberg series are included.*

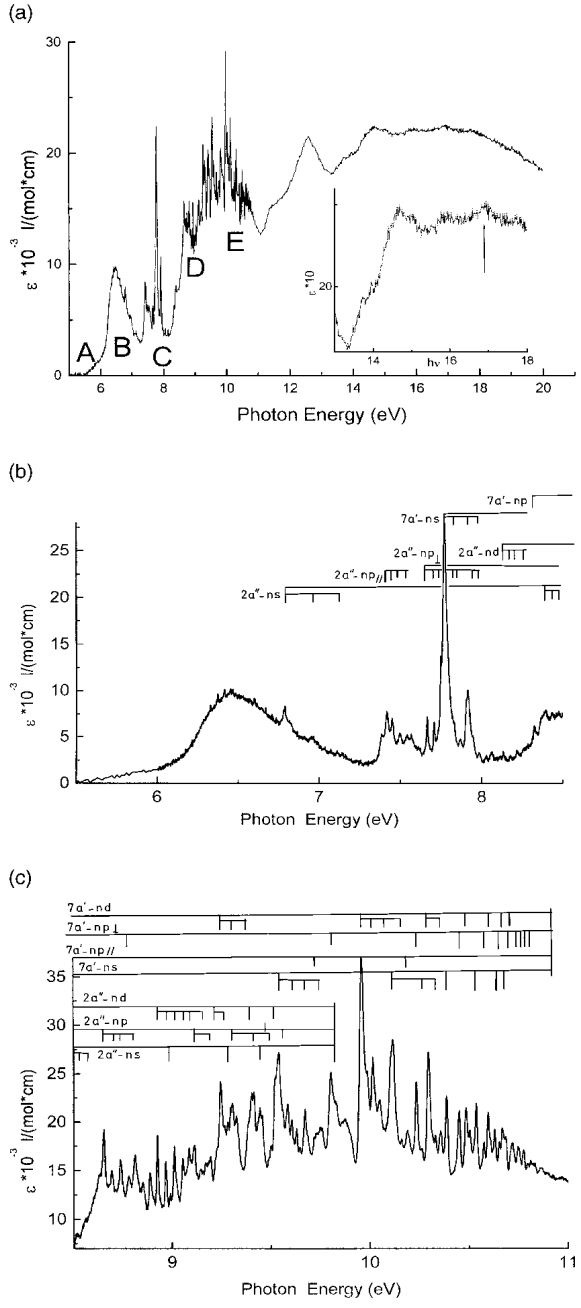

Published in: Chemical Physics (2000), vol. 260, pp. 237-243.
Status: Postprint (Author's version)

4. 2. The constant ion state spectra

The CIS spectra of fifteen vibrational levels of the first photoelectron band ($\tilde{X}^2A''$ state) and three vibrational levels of the $\tilde{A}^2A'$ state have been recorded up to an energy equal to 12 eV. They are shown in Fig. 3a-c. We also recorded the low resolution CIS spectra of the first six electronic states of the $C_2H_3Br^+$ ion up to an energy of about 22 eV, displayed in Fig. 4.

Fig. 3. *(a) and (b) CIS spectra corresponding to specified vibrational levels of $C_2H_3Br^+$ in the $\tilde{X}^2A''$ state and (c) in the A^2A'' state, at indicated photon energy.*

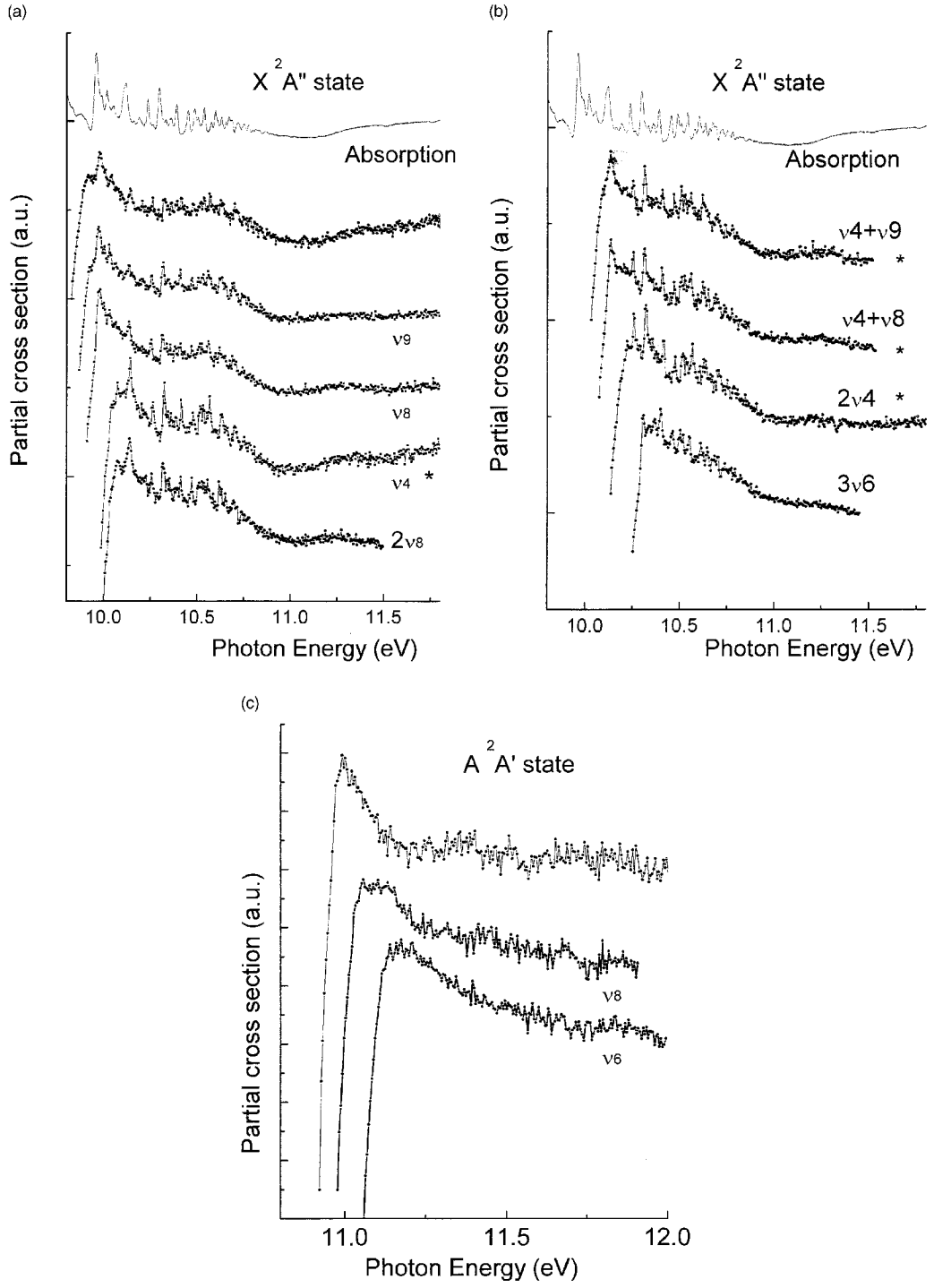

Published in: Chemical Physics (2000), vol. 260, pp. 237-243.
Status: Postprint (Author's version)

Fig. 4. *CIS spectra of the six first electronic states of $C_2H_3Br^+$.*

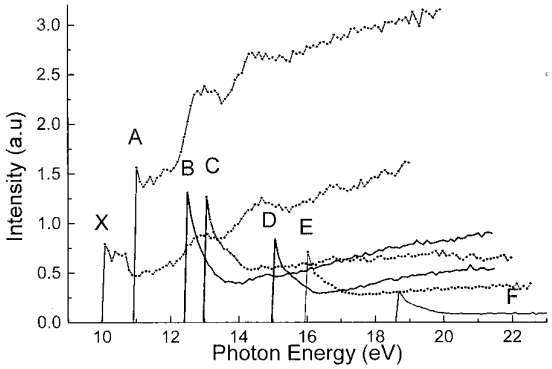

A first glance to these CIS spectra clearly shows a quite different shape of these curves. The CIS spectra corresponding to the vibrational levels of the $\tilde{X}^2A''$ state situated at energies lower than 10.314 eV exhibit sharp structures superimposed on a continuous background. On the contrary, the vibrational levels of the $\tilde{X}^2A''$ lying at energies higher than 10.314 as well as all vibrational levels corresponding to the $\tilde{A}^2A'$ state show a smooth decrease without any detectable structure up to 12.0 eV.

5. Discussion

In terms of valence molecular orbitals the ground state of $C_2H_3Br^+$ can be described as

$$\cdots (3a')^2(4a')^2(5a')^2(6a')^2(1a'')^2(7a')^2(2a'')^2\ \tilde{X}^1A'$$

The outermost occupied orbital corresponds to a π (C=C bonding, C-Br antibonding) orbital. The two next molecular orbitals can be, respectively, described as the in-plane bromine "lone pair" (7a") and the out-of-plane bromine "lone pair" (1a"), the latter possessing a certain C-Br bonding character.

5. 1. The valence transitions

The photoabsorption spectrum of C_2H_3Br contains sharp structured regions as well as several overlapping broad diffuse bands. This is clearly shown in Fig. 2b and c displaying the most structured part of the spectrum. The main broad bands observed here have been ascribed to valence to valence transitions. However, there has been some controversy in their assignment. In comparison with data on chloroethylene, Schander and Russel [3] attributed the intense broad band with a maximum near 6.5 eV to a $\pi \rightarrow \pi^*$ transition. It must be mentioned that the domain they investigated extends from 5.9 to 11 eV. Robin [15] reanalyzed their spectrum and assigned this band to a $\pi \rightarrow \sigma^*$ transition. Electron energy loss spectra starting from 5 eV revealed a small band at 5.7 eV attributed by Sze et al. to the $\pi \rightarrow \sigma^*$ transition [5]. These authors then reassigned the band at 6.5 eV to the $\pi \rightarrow \pi^*$ transition and analyzed the valence to valence transitions assuming transferability of term values. As previously mentioned, in order to obtain a better picture of the valence to valence transitions, we performed ab initio calculations for the fundamental and the first excited states of the C_2H_3Br molecule.

Table 1: *Excitation energies and oscillator strengths obtained from ab initio calculations*[a]

Transition	State symmetry	ΔE_{exc}[b] (eV)	Oscillator strength[c] (a. u.)
$\pi \rightarrow \sigma^*$	$^1A''$	6.4	0.0015
$n \rightarrow \sigma^*$	$^1A'$	7.3	0.0096
$\pi \rightarrow \pi^*$	$^1A'$	7.8	0.49
$n \rightarrow \pi^*$	$^1A''$	7.9	Very weak

[a] n represents the 7a' orbital (bromine in plane lone pair) and π, the 2a" orbital (C=C bonding, C-Br antibonding).
[b] From CASSCF calculations.
[c] From CIS calculations (see Section 3).

The main results concerning the excitation energies and the oscillator strengths are listed in Table 1. It should be mentioned that the calculated absolute excitation energies are higher than the experimental values, only their relative positions are relevant here. These relative positions are in agreement with previous results of Michl [6] who found that the first two singlet states correspond to the $\pi \rightarrow \sigma^*$ and the $n \rightarrow \sigma^*$ transitions and

Published in: Chemical Physics (2000), vol. 260, pp. 237-243.
Status: Postprint (Author's version)

mentions that the $\pi \rightarrow \pi^*$ state lies higher in energy. An important point comes out considering column 4 of Table 1: the oscillator strengths associated with the excitations to ^{1}A" states are extremely weak. Therefore we confidently assign the first weak band at 5.7 to the $n \rightarrow \sigma^*$ transition and the intense band at 6.5 eV to the $\pi \rightarrow \pi^*$ transition. Neglecting the transitions to ^{1}A" states and assuming a crude transferability of term values, the term scheme shown in Fig. 5 is obtained which leads to the assignments proposed in Table 2.

Table 2: *Observed and predicted valence to virtual valence transitions*[a]

Observed energies	Predicted energies[b]	Assignment
7.7	7.74	6a' → σ*
8.7	8.98	la" → π*
9.8	9.8	5a' → σ*
11.4	11	4a' → σ*

[a] Energies are given in eV.
[b] Predicted according to the term scheme given in Fig. 5.

Fig. 5. *Term scheme and predicted term values of valence to virtual valence transitions in C2H3Br between 6. 3 and 12. 0 eV photon energy.*

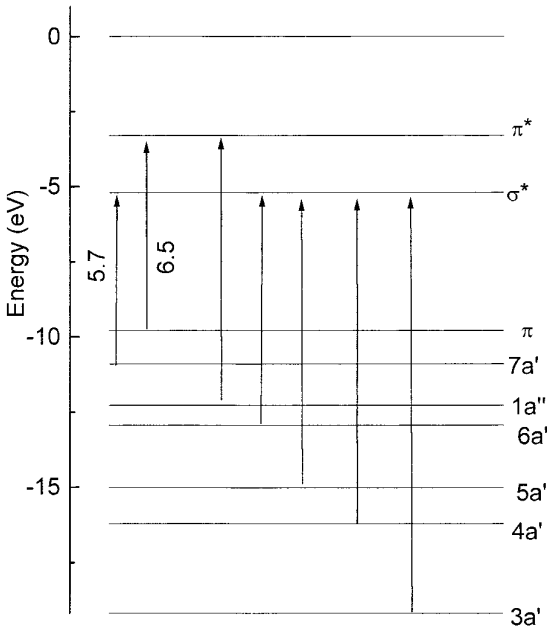

5. 2. The Rydberg transitions

Most of the sharp features observed between 6.5 and 11 eV were assigned to neutral Rydberg states converging to the first or the second ionization threshold. Their energies, E_{Rydb}, can be classified in series according to

$$E_{Rydb} = \text{IE} - R/(n - \delta)^2, \qquad (1)$$

where IE is the ionization energy, R, the Rydberg constant (13.6058 eV), n, the principal quantum number and δ, the quantum defect associated with the Rydberg state. The ionization energies we used are 9.804 and 10.899 eV, respectively, for the ground and first excited state of the ion as determined by photoelectron spectroscopy [1]. The value of $n - \delta$, also denoted by n^*, is related to the degree of penetration of the Rydberg electron into the quasi-ionic core, an effect related to the nature of the Rydberg orbital involved.

The fairly good resolution achieved in this work allowed us to identify three Rydberg series converging on the first ionization energy, as listed in Table 3. Only two of them have been described in the literature. According to the values of the quantum defects, we ascribed them to 2a" → *n*s and 2a" → *n*p and 2a" → *n*d transitions. For the lowest member of the 2a" → *n*p series two of the three possible transitions could be distinguished. The one characterized by the higher term value was assigned to $np_{\|}$ (a' symmetry) in agreement with the results of the study of the perfluoro effect [16]. For the higher members, only one 2a" → *n*p transition

could be found, probably indicating that the Rydberg electron experiences a highly symmetrical field from the ionic core.

Vibrational progressions belonging to these Rydberg transitions are also listed in Table 3. Their attribution is based on the constancy of the effective quantum number n^* for vibrational progressions in the same Rydberg state. No possibility for comparison exists because almost no vibrational structure of these series is presented in the literature. However, the observed wave numbers in the Rydberg states are close to the respective wave numbers in the $\tilde{X}^2A''$ ionic state (Table 4). Based on ab initio calculations reported in the analysis of the photoelectron spectra of C_2H_3Br [1], the following assignments can be proposed. The 335 ± 30 cm^{-1} (42 meV) wave number corresponds to the ν_9 mode (CH_2 rocking, with a small component on the C-Br stretching), whereas the 690 ± 30 cm^{-1} (86 meV) wave number can be assigned to the ν_8 mode (mainly a C-Br stretching). The remaining 1305 ± 30 cm^{-1} (162 meV) wave number is almost equal to its value in the ion (1315 cm^{-1}) and has been assigned to the ν_4 mode (CH_2 scissoring and C=C stretching). The geometrical changes occurring upon the involved transitions are compatible with the above mentioned vibrational motion descriptions [1].

Table 3: *Rydberg series converging towards the first ionization energy*

Limit	Assignment	Series							
		2a"-*n*s		2a"-*n*p		2a"-*n*p		2a"-*n*d	
		Energy	*n**	Energy	*n**	Energy	*n**	Energy	*n**
9.804	0	6.789	2.1243	7.666	2.5226	7.416	2.3869	8.131	2.8517
9.85	ν_9			7.709	2.5209	7.449	2.3804	8.177	2.8517
9.893	ν_8			7.75	2.5197	7.495	2.3819	8.222	2.8534
9.946	ν_6			7.793	2.5138	7.542	2.379	8.262	2.8424
9.968	ν_4	6.949	2.1229	7.831	2.5232				
10.011	$\nu_4 + \nu_9$			7.869	2.5200				
10.074	$3\nu_8$			7.944	2.5274				
10.14	$2\nu_6 + \nu_9$	7.111	2.1194	7.986	2.5133				
9.804	0	8.39	3.1019	8.653	3.4381			8.925	3.9343
9.85	ν_9	8.433	3.0986	8.694	3.4307			8.968	3.9276
9.893	ν_8	8.476	3.0986	8.737	3.4307			9.01	3.9253
9.946	ν_6	8.52	3.0888					9.053	3.9033
9.968	ν_4	8.554	3.1019	8.814	3.4336			9.087	3.9298
10.011	$\nu_4 + \nu_9$	8.851	3.4248						
10.035	$\nu_6 + \nu_8$	8.887	3.4426					9.145	3.9099
10.14	$2\nu_6 + \nu_9$							9.165	3.9410
9.804	0	8.992	4.0934	9.112	4.4341			9.223	4.839
9.85	ν_9							9.266	4.8267
9.893	ν_8			9.196	4.4182				
9.804	0	9.28	5.09561	9.325	5.3296			9.403	5.8249
9.893	ν_8			9.414	5.3296				
9.968	ν_4			9.499	5.3861				
9.804		9.444	6.14767	9.489	6.5721			9.52	6.9309
9.804				9.559	7.4521			9.585	7.8821
9.850								9.630	7.8641

Three Rydberg series converging towards the $\tilde{A}^2A'$ ionic state were identified. The suggested assignments, given in Table 5, are coherent with the analysis proposed by Lohr et al. [4] though they differ somewhat from those given by Sze et al. [5]. However, it must be remembered that the resolution achieved in this work is higher than that in earlier studies. Many previously unobserved structures have been analyzed, providing thus a stronger basis for the proposed assignments. The observed vibrational structures lead to wave numbers of 485 ± 30 cm^{-1} (60 meV) assigned to the ν_8 mode described by the C-Br stretching and 1145 ± 50 cm^{-1} (142 meV) attributed to the ν_6 mode described by a combination of C=C stretching and H-C-C-H bending motions. These values are in good agreement with those given by Lohr et al. [4], 484 and 1204 cm^{-1}, and the results of our own photoelectron spectroscopic study and ab initio calculations [1].

There remain some few weak and sharp peaks that could not be assigned. Their energy position is also given at the end of Table 5.

Published in: Chemical Physics (2000), vol. 260, pp. 237-243.
Status: Postprint (Author's version)

Table 4: *Vibrational wave numbers (in cm^{-1}) of the neutral, Rydberg states of C_2H_3Br and the first two ionic states of $C_2H_3Br^+$*

Mode	Neutral[a]	$\tilde{X}^2A'$ ionic state		$\tilde{A}^2A''$ ionic state	
		PES[b]	This work	PES[b]	This work
ν_9 (A')	344	380	335 ± 30	280	
ν_8 (A')	613	710	690 ± 30	460	485 ± 30
ν_6 (A')	1256	1145		1180	1145 ± 50
ν_4 (A')	1604	1315	1305 ± 30		
ν_3 (A')	3027	2540			

[a] From Ref. [19]. [b] From Ref. [1].

Table 5: *Rydberg series converging towards the second ionization energy and remaining unassigned peaks*

Limit	Assignment	Series							
		7a'-*n*s		7a'-*n*p		7a'-*n*p		7a' -*n*d	
		Energy	*n**	Energy	*n**	Energy	*n**	Energy	*n**
10. 899	0	7. 775	2. 0869	8. 781	2. 5345	8. 326	2. 2995	9. 244	2. 8672
10. 956	ν_8	7. 831	2. 0865					9. 305	2. 8707
11. 045	ν_6	7. 917	2. 0855					9. 387	2. 8646
11. 108	$\nu_6 + 2\nu_9$	7. 986	2. 0875						
10. 899	0	9. 541	3. 1652	9. 803	3. 5233	9. 715	3. 3898	9. 959	3. 8045
10. 956	ν_8	9. 606	3. 1746					10. 015	3. 8024
11. 045	ν_6	9. 673	3. 1490					10. 104	3. 8024
11. 108	$\nu_6 + 2\nu_9$	9. 748	3. 1629					10. 164	3. 7964
10. 899	0	10. 116	4. 1685	10. 236	4. 5300	10. 192	4. 3868	10. 296	4. 7501
10. 956	ν_8							10. 358	4. 7699
11. 045	ν_6	10. 264	4. 1738						
11. 108	$\nu_6 + 2\nu_9$	10. 332	4. 1872						
10. 899		10. 387	5. 1549	10. 452	5. 5170			10. 488	5. 7536
10. 899		10. 536	6. 1222	10. 575	6. 4802			10. 597	6. 7121
10. 899		10. 630	7. 1119	10. 654	7. 4521			10. 671	7. 7249
10. 899		10. 686	7. 9923	10. 707	8. 4180			10. 720	8. 7183
10. 899				10. 748	9. 4923				
10. 899				10. 776	10. 5174				
10. 899				10. 797	11. 5495				
10. 899				10. 813	12. 5780				
	?	7. 383							
	?	7. 567							
	?	7. 611							
	?	8. 029							
	?	8. 065							
	?	8. 110							
	?	9. 759							
	?	9. 826							
	?	10. 053							
	?	10. 501							

In addition, other structures are present at higher photon energies. Unlike the sharp Rydberg states related to the lower ionization energies, their shape is diffuse most probably due to very fast relaxation to lower states. A very tentative assignment is given in Table 6 where they have been interpreted as the first members of Rydberg series converging on higher ionization energies or as inner valence to virtual valence transitions.

5.3. Constant ion state spectra

All the CIS spectra of vibrationally resolved levels of the first electronic state show a important dip in the 11 eV region. The sharp structures observed in the vibrationally resolved partial cross sections of the ionic states situated below 10.314 eV will be analyzed in the next subsection. The CIS curves of the vibrational levels of the second electronic state ^{2}A' (Fig. 3c) show only a smooth decrease of the cross-section without any autoionisation contribution.

Table 6 : *Tentative assignment of some of the high energy features observed in the photoabsorption spectrum*

Observed energies (eV)	Tentative assignment	Ionization energy (eV)	Effective quantum number, n^*
11.4	4a' → σ*/3a' → *n*s/*n*d	18.7	1.35
12.6	4a' → *n*s/*n*d	16.02	1.99
13.7	3a' → σ*/4a' → *n*p	16.02	2.42
14.5	3a' → *n*p	18.7	1.76
16.8	3a' → *n*p	18.7	2.55

The low resolution CIS curve of the $\tilde{X}^2$A" ionic state presents several bands corresponding to the direct formation of the ground state of the ion by energetic photons. In agreement with the results of the He(I) and threshold photoelectron spectroscopy [1] the second electronic state ^{2}A' presents by far the most important relative cross-section. It also shows broad structures superimposed to an increasing background. The other electronic states only exhibit a smooth monotonic shape. It must also be noted that the peaked threshold behavior of all curves is an artifact due to the normalization procedure (see paragraph 2).

5. 3. 1. Analysis of the autoionization decay of Rydberg states

The fine structure observed in the CIS spectra of the $\tilde{X}^2$A" state can be assigned to the autoionization of neutral Rydberg states. Part of the absorption spectrum is displayed in top of Fig. 3a and b in order to show the one to one correspondence of these features to the members of the three Rydberg series converging towards the second ionization energy at 10.899 eV.

No correlation could be found between the intensities of the autoionization structures and the type of the orbital involved in the excitation of the neutral. However, a close examination of the present CIS spectra reveals that the autoionization features are more emphasized in the partial cross-sections of the vibrational states involving excitation of the ν_4 mode (marked with an asterisk in Fig. 3a and b). The other CIS profiles corresponding to the excitation of the ν_8 and ν_9 modes, including the vibrationless level, exhibit less pronounced autoionization structures.

We have tried to rationalize the above observation using a simple model initially proposed for the analysis of the photoionisation dynamics of 1,1 difluoroethylene [17]. In the framework of the Franck-Condon approximation, the autoionization contribution to the intensities of the CIS spectra will, in a first approximation, be related to the product of two Franck-Condon factors, the first one governing the excitation transition from the neutral to the Rydberg state and the second corresponding to the overlap integral between the Rydberg state and the vibrational state of the ion [18]:

$$I \approx |\langle 0^{\text{ground}}_{\text{state}} | \chi^{\text{Ry}} \rangle|^2 \, |\langle \chi^{\text{Ry}} | \chi^{\text{ion}}_{\text{X state}} \rangle|^2, \qquad (2)$$

where $|0\rangle$ represents the vibrationless wave function (of the neutral ground state in this case) and $|\chi\rangle$, the vibrational wave function of the ionic or Rydberg state (as defined in the upper index).

In our case, from the assignments proposed in Table 5, it becomes clear that all the Rydberg states involved correspond to a vibrationless core:

$$I \approx |\langle 0^{\text{ground}}_{\text{state}} | 0^{\text{Ry}} \rangle|^2 \, |\langle 0^{\text{Ry}} | \chi^{\text{ion}}_{\text{X state}} \rangle|^2. \qquad (3)$$

The first factor also controls the intensities in the photoabsorption spectrum. This explains why all the CIS spectra mimic the absorption spectrum (Fig. 3a and b).

From the second integral, it can be inferred that the branching ratios for the decay of a given Rydberg

state will depend on the vibrational level of the final ionic state.

As far as relatively high Rydberg states are concerned, their geometry (and wave functions) are expected to be relatively well represented by the geometry (and wave functions) of the first excited state of the ion. With this assumption, the second integral can be written:

$$|\langle 0^{\text{ion}}_{A\,\text{state}} | \chi^{\text{ion}}_{X\,\text{state}} \rangle|^2 \qquad (4)$$

We can now refer to the results of the analysis of the photoelectron spectra to estimate the influence of the ionic ground-state vibrational level on this integral. According to ab initio calculations and in agreement with photoelectron spectroscopy results, [1], the equilibrium normal coordinates corresponding to the ν_8 and ν_9 modes are shorter for the $\tilde{X}^2A''$ ionic state than for the ground state of the neutral, while the reverse is true for the $\tilde{A}^2A'$ ionic state. In such a situation, the overlap integral (4) is expected to be vanishing. On the contrary, the ν_4 mode is not excited in the photoelectron spectrum of the $\tilde{A}^2A'$ state, leading to the conclusion that the corresponding normal coordinate is not changed with respect to its value in the neutral. The relatively rich ν_4 progression observed in the photoelectron spectrum of the $\tilde{X}^2A''$ state directly confirms that overlap integral of the ground state of the neutral and of vibrational factors corresponding to the excitation of the ν_4 mode of the $\tilde{X}^2A''$ ionic state is important. As a result, the overlap integral (4) will be important when the $\tilde{X}^2A''$ vibrational states involve excitation of the ν_4 mode. This leads to larger partial cross-sections as observed experimentally.

It must be noticed that this qualitative analysis also explains the very high intensity of the 0-lν_4 transition (vertical) in the TPES spectrum of the $\tilde{X}^2A''$ state with respect to its intensity in the He(I) spectrum [1].

6. Conclusion

The photoabsorption spectrum of C_2H_3Br investigated with the help of synchrotron radiation has been analyzed in terms of valence to virtual valence and Rydberg transitions. Ab initio calculations helped with the assignment of the first valence to virtual valence transitions. In comparison with previous work, extended vibrational structures have been identified at least for the low members of the Rydberg series. The assignments of the observed vibrational structures are in agreement with the results of previous ab initio calculations [1].

The vibrationally resolved partial cross-sections of the $\tilde{X}^2A''$ state of the $C_2H_3Br^+$ ion give evidence for the importance of autoionization for vinylbromide. It is observed that the CIS spectra of levels involving excitation of the ν_4 mode of the $\tilde{X}^2A''$ ionic state present more pronounced autoionization structures. The influence of the final state vibrational level has been analyzed in terms of Franck-Condon factors between the Rydberg and the ionic state.

Acknowledgements

We are indebted to the University of Liège, the Freie Universität Berlin and the Bundesministe-rium für Forschung und Technologie for financial support. This work has been supported by the Actions de Recherche Concertée (ARC) (Direction de la Recherche Scientifique - Communauté Française de Belgique). A.H., R.L. and B.L. acknowledge the European Community for financing this work through its Human Capital and Mobility Programme (Contract no. ERBFMGE-CT 97-0123). B.L. is indebted to the F.N.R.S. (Belgium) for a research associate position. D.D.'s contribution was supported by the Belgian Program of Pôles d'Attraction Interuniversitaires (PAI no. P4/03) initiated by the Belgian state, the Prime Minister's Office, the Federal Office of Scientific, Technical and Cultural Affairs. Financial support of the Fonds des Chemischen Industrie is gratefully acknowledged by H.B. We also wish to thank the BESSY I staff for the outstanding maintenance of the equipment.

References

[1] A. Hoxha, R. Locht, B. Leyh, D. Dehareng, K. Hottmann, H. Baumgärtel, Chem. Phys. 256 (2000) 239.

[2] A. Hoxha, R. Locht, A.J. Lorquet, J.C. Lorquet, B. Leyh, J. Chem. Phys. 111 (1999) 9259.

[3] J. Schander, B.R. Russell, J. Am. Chem. Soc. 98 (1976) 6900.

[4] W. Lohr, H.W. Jochims, H. Baumgärtel, Ber Bunsen-Gesell 79 (1975) 901.

[5] K.H. Sze, C.E. Brion, A. Katrib, B. El-Issa, Chem. Phys. 137 (1989) 369.

[6] J. Michl, V. Bonačić-Kontecký, Electronic Aspects of Organic Photochemistry, Wiley, New York, 1990.

[7] K. Hottmann, H.-W. Jochims, H. Baumgärtel, Bessy Jahresbericht, 1987, 398.

[8] R. Locht, B. Leyh, K. Hottmann, H. Baumgärtel, Chem. Phys. 220 (1997) 217.

[9] M.J. Frisch, G.W. Trucks, H.B. Schlegel, P.M.W. Gill, B.G. Johnson, M.A. Robb, J.R. Cheeseman, T.A. Keith, G.A. Petersson, J.A. Montgomery, K. Raghavachari, M.A. Al-Laham, V.G. Zakrzewski, J.V. Ortiz, J.B. Fores-man, J. Cioslowski, B.B. Stefanov, A. Nanayakkara, M. Challacombe, C.Y. Peng, P.Y. Ayala, W. Chen, M.W. Wong, J.L. Andres, E.S. Replogle, R. Gomperts, R.L. Martin, D.J. Fox, J.S. Binkley, D.J. Defrees, J. Baker, J.P. Stewart, M. Head-Gordon, C. Gonzalez, J.A. Pople, GAUSSIAN 94 (Revision D. 4), Gaussian Inc., Pittsburg, 1996.

[10] D. Hegarty, M.A. Robb, Mol. Phys. 38 (1979) 1795.

[11] J.B. Foresman, M. Head-Gordon, J.A. Pople, M.J. Frisch, J. Phys. Chem. 96 (1992) 135.

[12] A.D. McLean, G.S. Chandler, J. Chem. Phys. 72 (1980) 5639.

[13] T. Clark, J. Chandrasekhar, G.W. Spitznagel, P.v.R. Shleyer, J. Comp. Chem. 4 (1983) 294.

[14] M.J. Frisch, J.A. Pople, J.S. Binkley, J. Chem. Phys. 80 (1984) 3265.

[15] M.B. Robin, Higher Excited States of Polyatomic Molecules, Academic Press, New York, 1974.

[16] J. Schander, B.R. Russell, J. Mol. Spectrosc. 65 (1977) 379.

[17] B. Leyh, R. Locht, K. Hottmann, H. Baumgärtel, submitted for publication.

[18] A.L. Smith, Phil. Trans. R. Soc. Lond. A 268 (1970) 169.

[19] S.A. Abrash, R.W. Zehner, G.J. Mains, L.M. Raff, J. Phys. Chem. 99 (1995) 2959.